Solubility Investigations in the Systems $K_2B_4O_7 + Li_2B_4O_7 + H_2O$ and $Na_2B_4O_7 + Li_2B_4O_7 + H_2O$ at $T = 288$ K

Shi-hua Sang,* Hui-an Yin, Ming-lin Tang, and Ning-Fei Lei

Department of Applied Chemistry, Chengdu University of Technology, Chengdu 610059, China

The solubility of the salt and the density, electrical conductivity, and pH of ternary systems $K_2B_4O_7 + Li_2B_4O_7 + H_2O$ and $Na_2B_4O_7 + Li_2B_4O_7 + H_2O$ at $T = 288$ K were determined. On the basis of the experimental results, phase diagrams and property composition diagrams were derived. Phase equilibrium solids were $Na_2B_4O_7{\cdot}10H_2O$, $K_2B_4O_7{\cdot}4H_2O$, and $Li_2B_4O_7{\cdot}3H_2O$. Analyses of what was made on the crystallization areas in the phase diagram were discussed. The results of properties in the solution were also discussed simply.

Introduction

Salt lake brines of high concentration contain abundant mineral resources. To exploit brine resources, mineral equilibrium studies on the brines at different temperatures are necessary. There are many salt lakes in China, especially on the Qinghai−Tibet plateau.[1] In Tibet, many salt lakes have been found that have distinct characteristics from others and are famous for the highest concentrations of lithium, potassium, and boron in the world. Of all of the salt lakes in Tibet, the Zhabuye salt lake has distinct characteristics from others, with an area of 240 km^2, and is famous for the highest concentrations of lithium, boron, and potassium in the world. The main components are Li^+, K^+, Na^+, Rb^+, Cs^+, $B_4O_7^{2-}$, CO_3^{2-}, Cl^-, SO_4^{2-}, and H_2O. The proven resources of lithium, potassium, and boron are huge.[2] To exploit these salt lake brines, some mineral equilibrium ternary systems have been studied at $T = 298$ K.[3,4] Some studies have been done on the solubility of the $K_2B_4O_7 + Na_2B_4O_7 + H_2O$ system at $T = 288$ K.[5] Single borate solubilities at different temperatures have been reported.[6] Furthermore, the prediction of some borate mineral equilibria without lithium borate in natural water have also been made for the Searles salt lake.[7] The ternary systems are subsystems of Zhabuye salt lake brines, which are the basis of quaternary and quinary phase equilibria for the brines. To this day, however, equilibrium experimental studies for the $K_2B_4O_7 + Li_2B_4O_7 + H_2O$ and $Na_2B_4O_7 + Li_2B_4O_7 + H_2O$ systems at $T = 288$ K have not been reported.

In this paper, the phase equilibria and physicochemical properties of equilibrium solutions (pH, density, and electrical conductivity) for the ternary systems listed above are studied experimentally.

Experimental Section

Reagents. All chemicals used were of analytical-grade purity, that is, $K_2B_4O_7{\cdot}5H_2O$, $Li_2B_4O_7$, and $Na_2B_4O_7{\cdot}10H_2O$. The electrical conductivity of distilled water was less than 1×10^{-4} $S{\cdot}m^{-1}$ at pH 6.6.

Instruments. An HZS-H-type thermostated vibrator with an uncertainty of 0.1 K was used for the equilibrium measurement. A PHS-3C digital acidometer with an uncertainty of 0.01 was used for pH values of equilibrium solutions. A DDZ-11A-type conductometer with an uncer-

* To whom correspondence should be addressed. E-mail:sangsh@cdut.edu.cn.

Table 1. Solubility, Density ρ, and Electrical Conductivity κ of a Solution in the Ternary System $K_2B_4O_7$(1) + $Li_2B_4O_7$ (2) + H_2O(3) at $T = 288$ K[a]

$100w_1$	$100w_2$	ρ/(g cm^{-3})	κ/(S m^{-1})	pH	solid phase
0	2.55	1.0193	0.75	9.62	$Li_2B_4O_7{\cdot}3H_2O$
0.15	2.59	1.0199	0.80	9.73	$Li_2B_4O_7{\cdot}3H_2O$
1.40	2.54	1.0218	1.06	9.75	$Li_2B_4O_7{\cdot}3H_2O$
3.58	2.42	1.0239	1.45	9.82	$Li_2B_4O_7{\cdot}3H_2O$
6.19	2.35	1.0462	1.82	9.85	$Li_2B_4O_7{\cdot}3H_2O$
8.15	2.27	1.0649	1.95	9.93	$Li_2B_4O_7{\cdot}3H_2O$
8.60	2.25	1.0698	2.15	9.96	$Li_2B_4O_7{\cdot}3H_2O$
8.65	2.19	1.0654	2.33	10.00	$Li_2B_4O_7{\cdot}3H_2O$
9.11	2.18	1.0942	2.45	10.02	$Li_2B_4O_7{\cdot}3H_2O$
10.54	2.09	1.1215	2.75	10.03	$Li_2B_4O_7{\cdot}3H_2O$ + $K_2B_4O_7{\cdot}4H_2O$
10.56	1.90	1.1197	2.74	10.01	$K_2B_4O_7{\cdot}4H_2O$
10.77	1.46	1.1136	2.75	10.02	$K_2B_4O_7{\cdot}4H_2O$
10.82	1.17	1.1090	2.74	10.02	$K_2B_4O_7{\cdot}4H_2O$
11.49	0.77	1.0978	2.72	10.01	$K_2B_4O_7{\cdot}4H_2O$
11.52	0.0	1.0972	2.70	10.02	$K_2B_4O_7{\cdot}4H_2O$

[a] w represents mass fraction.

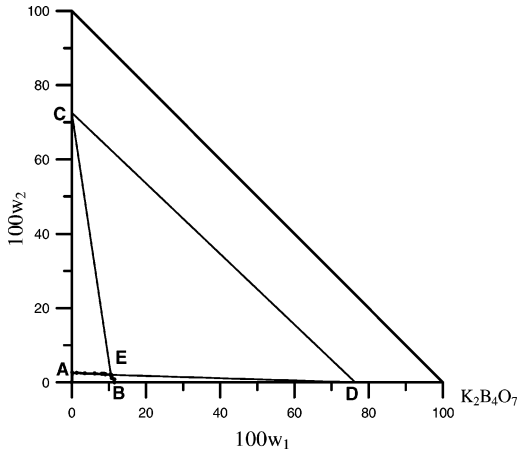

Figure 1. Phase diagram of the ternary system $K_2B_4O_7$(1) + $Li_2B_4O_7$(2) + H_2O(3) at 288 K. Experimental data points: A, binary system $Li_2B_4O_7 - H_2O$ saturation point; B, binary system ($K_2B_4O_7 - H_2O$) saturation point; C, solid-phase point ($Li_2B_4O_7{\cdot}3H_2O$); D, solid-phase point ($K_2B_4O_7{\cdot}4H_2O$); E, invariant point saturated with $Li_2B_4O_7{\cdot}3H_2O$ and $K_2B_4O_7{\cdot}4H_2O$.

10.1021/je034280k CCC: $27.50
Published on Web 10/14/2004

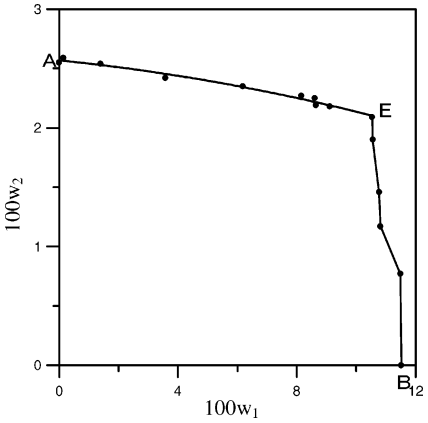

Figure 2. Enlarged partial phase diagram of the ternary system $K_2B_4O_7(1) + Li_2B_4O_7(2) + H_2O(3)$ at 288 K. Experimental data points: A, binary system $Li_2B_4O_7 - H_2O$ saturation point; B, binary system ($K_2B_4O_7 - H_2O$) saturation point; E, invariant point saturated with $Li_2B_4O_7{\cdot}3H_2O$ and $K_2B_4O_7{\cdot}4H_2O$.

Table 2. Solubility, Density ρ, and Electrical Conductivity κ of a Solution in the Ternary System $Na_2B_4O_7$ (1) + $Li_2B_4O_7$ (2) + H_2O(3) at 288 K[a]

$100w_1$	$100w_2$	ρ/(g cm^{-3})	κ/(S m^{-1})	pH	solid phase
2.13	0	1.0181	0.71	9.67	$Na_2B_4O_7{\cdot}10H_2O$
1.94	0.40	1.0201	0.79	9.64	$Na_2B_4O_7{\cdot}10H_2O$
1.84	0.68	1.0216	0.82	9.66	$Na_2B_4O_7{\cdot}10H_2O$
1.75	0.98	1.0235	0.86	9.65	$Na_2B_4O_7{\cdot}10H_2O$
1.66	1.10	1.0249	0.86	9.69	$Na_2B_4O_7{\cdot}10H_2O$
1.58	1.61	1.0285	0.92	9.74	$Na_2B_4O_7{\cdot}10H_2O$
1.52	1.69	1.0297	0.99	9.74	$Na_2B_4O_7{\cdot}10H_2O$ + $Li_2B_4O_7{\cdot}3H_2O$
1.45	1.68	1.0265	0.86	9.70	$Li_2B_4O_7{\cdot}3H_2O$
1.39	1.66	1.0259	0.85	9.69	$Li_2B_4O_7{\cdot}3H_2O$
1.26	1.76	1.0237	0.82	9.67	$Li_2B_4O_7{\cdot}3H_2O$
0.83	2.02	1.0209	0.82	9.65	$Li_2B_4O_7{\cdot}3H_2O$
0.68	2.18	1.0198	0.81	9.65	$Li_2B_4O_7{\cdot}3H_2O$
0	2.55	1.0193	0.75	9.62	$Li_2B_4O_7{\cdot}3H_2O$

[a] w represents mass fraction.

tainty of 0.01 S·m^{-1} was used for the electrical conductivity values of equilibrium solutions.

Experimental Method. The experiments for phase equilibria were done by the method of isothermal solution saturation. The system points for the ternary system were compounded by adding the second component gradually on the basis of the single-salt saturation points at 288 K. Then the mixed brines were poured into a sealed tube and placed in the thermostated vibrator (HZC-H). The sealed tubes with solution were stirred for 1 week. The time of clarification was about 5 days. The solutions were taken out periodically for chemical analysis. When the components of the solution did not change, the equilibria were finished. After equilibrium was reached, the liquid phases were taken out and subjected to quantitative analysis, and the solid phases were separated at the corresponding temperature. After the wet-residue mixture was filtered out, wet crystals were separated from each other according to crystal shapes as much as possible. Then solids were approximately evaluated by chemical analysis for wet residues; further identification was done by X-ray diffraction.

The pH values and electrical conductivity values of the equilibrium solutions were measured by the corresponding listed instruments. The densities of solution were determined by a specific graving bottle method with a correction for the floating force of air with an uncertainty of 0.0001 g·cm^{-3}.[8]

Analytical Methods.[8] The potassium ion concentration was measured by sodium tetraphenylborate-hexadecyltrimethylammonium bromide titration (uncertainty of 0.5 mass %). The borate ion concentration was evaluated by basic titration with the existence of mannitol (uncertainty of 0.3 mass %). The lithium ion concentration was determined by atomic absorption spectrophotometry (AAS), and the sodium ion concentration was evaluated according to ion balance. The relative error of the determination of the concentration of the lithium ion was estimated to be less than 1%.

Results and Discussion

$K_2B_4O_7 + Li_2B_4O_7 + H_2O$ System. The experimental results of the solubilities and physicochemical properties (pH, density and electrical conductivity) for the $K_2B_4O_7 + Li_2B_4O_7 + H_2O$ ternary system at $T = 288$ K were determined and tabulated in Table 1. The respective ion concentration values were expressed in mass fraction. The solution density (ρ) is given in grams per centimeter, and the electrical conductivity (κ) is given siemens per meter. The corresponding phase diagram was plotted in Figure 1. Figure 2 is the enlarged partial phase diagram. Figures

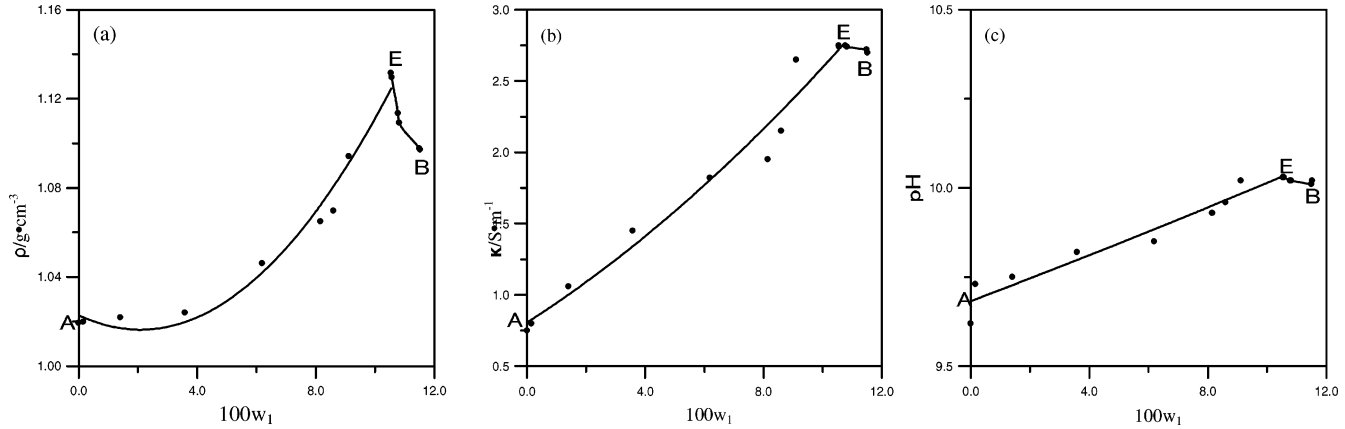

Figure 3. Physicochemical property−composition diagram for the ternary system $K_2B_4O_7(1) + Li_2B_4O_7(2) + H_2O(3)$ at 288 K. Experimental data points: AE, physicochemical property values (density, electrical conductivity, and pH) corresponding to univariant curves AE; BE, physicochemical property values (density, electrical conductivity, and pH) corresponding to univariant curve BE; E, physicochemical property value corresponding to invariant point E. (a) Density−composition diagram. (b) Electrical conductivity−composition diagram. (c) pH−composition diagram.

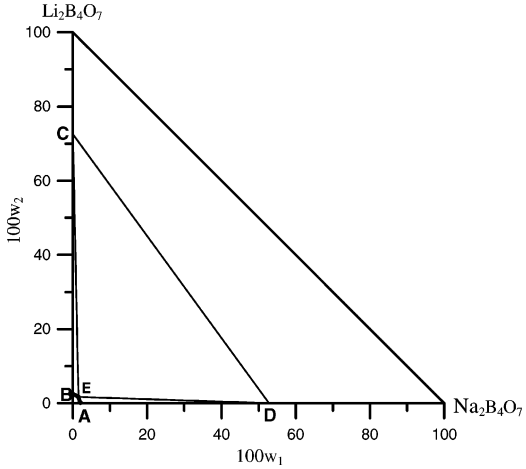

Figure 4. Phase diagram of the ternary system $Na_2B_4O_7$(1) + $Li_2B_4O_7$(2) + H_2O(3) at 288 K. Experimental data points: A, binary system ($Na_2B_4O_7$ − H_2O) saturation point; B, binary system ($Li_2B_4O_7$ − H_2O) saturation point; C, solid-phase point ($Li_2B_4O_7$·$3H_2O$); D, solid-phase point ($Na_2B_4O_7$·$10H_2O$); E, invariant point saturated with $Li_2B_4O_7$·$3H_2O$ and $Na_2B_4O_7$·$10H_2O$.

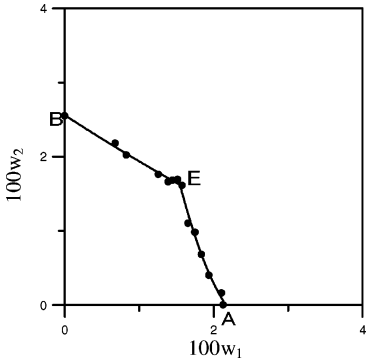

Figure 5. Enlarged partial phase diagram of the ternary system $Na_2B_4O_7$(1) + $Li_2B_4O_7$ (2) + H_2O(3) at 288 K. Experimental data points: A, binary system ($Na_2B_4O_7$ − H_2O) saturation point; B, binary system ($Li_2B_4O_7$ − H_2O) saturation point; E, invariant point saturated with $Li_2B_4O_7$·$3H_2O$ and $Na_2B_4O_7$·$10H_2O$.

1 and 2 show that there are two single-salt crystallization zones for $K_2B_4O_7$·$4H_2O$(BED) and $Li_2B_4O_7$·$3H_2O$(AEC), one invariant point E, and two univariant curves AE and BE. The crystallization field for $Li_2B_4O_7$·$3H_2O$ in the phase diagram is larger than that of $K_2B_4O_7$·$4H_2O$. The AE and BE curves of the solubility isotherm in Figures 1 and 2 are linear. The $Li_2B_4O_7$ concentration with increasing increment of concentration of $K_2B_4O_7$ (AE curve) is diminishing toward the eutonic point (E). The monotonic course of the curves implies that no chemical compound is formed in the studied systems.

According to the experimental data of physicochemical properties, the property−composition diagrams are shown in Figure 3. Figure 3 shows that density values, pH values, and electrical conductivity values of the equilibrium solution increase with rising $K_2B_4O_7$ (for the saturated solutions of $Li_2B_4O_7$·$3H_2O$) concentration, reaching their maximum values at the eutonic point E. When these specific points are exceeded, these values for the density, pH, and electrical conductivity are decreased and reach a similar point (B) of solutions saturated with $K_2B_4O_7$·$4H_2O$.

NaB_4O_7 + $Li_2B_4O_7$ + H_2O System. The experimental results of the solubilities and physicochemical properties for the $Na_2B_4O_7$ + $Li_2B_4O_7$ + H_2O ternary system at 288 K are tabulated in Table 2; the corresponding phase diagrams are plotted in Figures 4 and 5.

The experimental results and Figures 4 and 5 show that there are two crystallization zones for $Na_2B_4O_7$·$10H_2O$-(AED) and $Li_2B_4O_7$·$3H_2O$(BEC), one invariant point E, and two univariant curves AE and BE. AE curves correspond to the solubility isotherms where the solution was saturated with $Na_2B_4O_7$·$10H_2O$. BE curves correspond to the solubility isotherms where the solution was saturated with $Li_2B_4O_7$·$3H_2O$. Eutonic point E corresponds to the solution saturated with $Na_2B_4O_7$·$10H_2O$ and $Li_2B_4O_7$·$3H_2O$.

The physicochemical property−composition diagrams are shown in Figure 6 on the basis of the experimental data of physicochemical properties.

Figure 6 shows that density values, pH values, and conductivity values of the equilibrium solution increase with increasing solution concentration. The largest values occur at saturation point E.

On the basis of the data collected Tables 1 and 2, relationships between the solution property pH and the logarithmic ion concentration values $\log(C_{B_4O_7})$ are finished in Figures 7 and 8. The curves are linear on the whole. It can be seen that in the systems the pH values of the solution depended on the concentration of $B_4O_7^{2-}$.

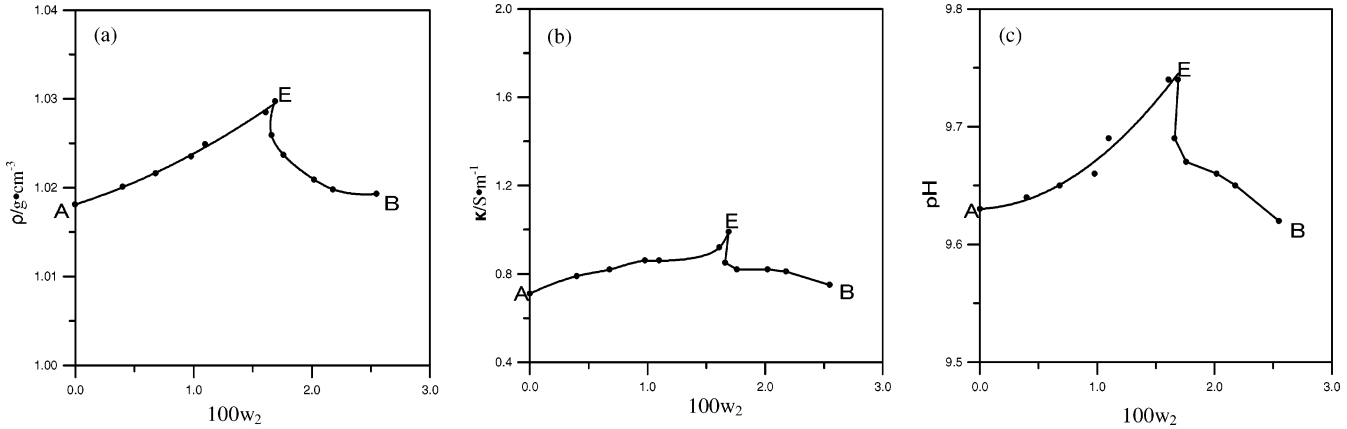

Figure 6. Physicochemical property−composition diagram for the ternary system, $Na_2B_4O_7$ (1) + $Li_2B_4O_7$(2) + H_2O(3) at 288 K. Experimental data points: AE, physicochemical property values (density, electrical conductivity, and pH) corresponding to univariant curves AE; BE, physicochemical property values (density, electrical conductivity, and pH) corresponding to univariant curve BE; E, physicochemical property value corresponding to invariant point E. (a) Density−composition diagram. (b) Electrical conductivity−composition diagram. (c) pH−composition diagram.

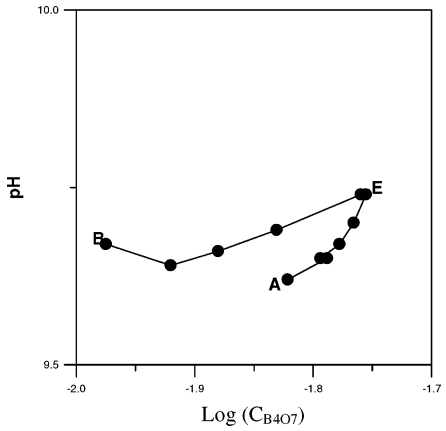

Figure 7. Relationship diagram between pH values and log($C_{B_4O_7}$) for the $Na_2B_4O_7 + Li_2B_4O_7 + H_2O$ system.

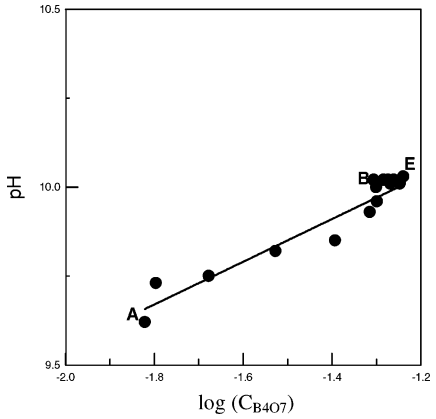

Figure 8. Relationship diagram between pH values and log($C_{B_4O_7}$) for the $K_2B_4O_7 + Li_2B_4O_7 + H_2O$ system.

Conclusions

The solubilities and the properties of the solution in the $K_2B_4O_7 + Li_2B_4O_7 + H_2O$ and $Na_2B_4O_7 + Li_2B_4O_7 + H_2O$ systems at $T = 288$ K were determined in this paper. According to the experimental data measured, phase diagrams and property−composition diagrams were constructed. The equilibrium solid phases for the $K_2B_4O_7 + Li_2B_4O_7 + H_2O$ system at 288 K are $K_2B_4O_7{\cdot}4H_2O$ and $Li_2B_4O_7{\cdot}3H_2O$. The equilibrium solid phase for the $K_2B_4O_7 + Li_2B_4O_7 + H_2O$ system at 288 K are $Na_2B_4O_7{\cdot}10H_2O$ and $Li_2B_4O_7{\cdot}3H_2O$. Simple discussions were made on the construction of the diagram.

Literature Cited

(1) Zheng, M. P.; Xiang, J. Salt lakes of Oinghai-Tibet plateau. *Science and Technology Press*: Beijing, 1989 (in Chinese).

(2) Zheng, X. Y.; Tang, Y.; Xu, Y. et al. Salt lakes of Tibet. *Science and Technology Press*: Beijing, 1988 (in Chinese).

(3) Sang, S. H.; Deng, T. L.; Tang, M. L.; Yin, H. A. Experimental Study of Solubilities and Properties of Solution in the System $Li_2B_4O_7$-$Na_2B_4O_7$-H_2O at 25 °C, *J. Chengdu Inst. Technol.* **1997**, *24*, 87−90.

(4) Yu, T.; Tang, M. L.; Deng, T. L.; Yin, H. A. An Experimental Study on the Solubility Diagram and Physicochemical Properties of Solution in the Ternary System $Li_2B_4O_7$-$K_2B_4O_7$-H_2O at 25 °C. *J. Mineral. Petrol.* **1997**, *17*, 105−109.

(5) Sang, S. H.; Tang, M. L.; Yin, H. A.; Zhang Y. X. A Study on Phase Equilibria for the Ternary System $K_2B_4O_7$-$Na_2B_4O_7$-H_2O at 288K. *J. Sea-Lake Chem. Ind.* **2002**, *31*, 16−18.

(6) Stephen, H.; Stephen, T. *Solubilities of Inorganic and Organic Compounds*; Pergamon Press: Oxford, U.K., 1979; Vol. 1.

(7) Felmy, A. R.; Weare, J. H. The Prediction of Borate Mineral Equilibria in Nature Waters: Application to Searles lake, Califonia, *Geochim. Cosmochim. Acta* **1986**, *50*, 2271−2783.

(8) Institute of Qinghai Salt-Lake, Chinese Academy of Science; *Analytical Methods of Brines and Salts*; Science Press: Beijing, 1988 (in Chinese).

Received for review December 22, 2003. Accepted August 30, 2004. The work was supported by the National Nature Science Foundation of China (no. 40303010).

JE034280K